Ultrabroadband efficient intracavity XUV output coupler

Oleg Pronin,[1,*] Vladimir Pervak,[2] Ernst Fill,[2] Jens Rauschenberger,[1,2] Ferenc Krausz,[1,2] and Alexander Apolonski[1,2]

[1]*Max-Planck-Institut für Quantenoptik, Hans-Kopfermann-Strasse 1, D-85748 Garching, Germany*
[2]*Ludwig-Maximilians-Universität München, Am Coulombwall 1, D-85748 Garching, Germany*
**oleg.pronin@mpq.mpg.de*

Abstract: We report an efficient intracavity XUV output coupler based on an anti-reflection-coated grazing incidence plate (GIP). Conceptually, GIP is an extension of a Brewster plate, affording low loss of the circulating fundamental light and serving as a highly efficient, extremely broadband output coupler for XUV. Due to the grazing incidence geometry, the short wavelength reflectivity can be extended to the keV range. The first GIP realized shows parameters close to the design. We discuss both the limitations of the GIP in comparison with other XUV output couplers and the applicability of the GIP extension at longer wavelengths, down to the MIR.

OCIS codes: (320.7110) Ultrafast nonlinear optics; (340.7480) X-rays, soft x-rays, extreme ultraviolet (EUV); (140.7240) UV, EUV, and x-ray lasers; (310.1210) Antireflection coatings; (310.4165) Multilayer design.

References and links

1. E. Goulielmakis, M. Schultze, M. Hofstetter, V. S. Yakovlev, J. Gagnon, M. Uiberacker, A. L. Aquila, E. M. Gullikson, D. T. Attwood, R. Kienberger, F. Krausz, and U. Kleineberg, "Single-cycle nonlinear optics," Science **320**(5883), 1614–1617 (2008).
2. M. Herrmann, M. Haas, U. Jentschura, F. Kottmann, D. Leibfried, G. Saathoff, C. Gohle, A. Ozawa, V. Batteiger, S. Knünz, N. Kolachevsky, H. Schüssler, T. Hänsch, and T. Udem, "Feasibility of coherent XUV spectroscopy on the 1*S*-2*S* transition in singly ionized helium," Phys. Rev. A **79**(5), 052505 (2009).
3. C. Spielmann, N. H. Burnett, S. Sartania, R. Koppitsch, M. Schnürer, C. Kan, M. Lenzner, P. Wobrauschek, and F. Krausz, "Generation of coherent X-rays in the water window using 5-femtosecond laser pulses," Science **278**(5338), 661–664 (1997).
4. A. Ashkin, G. D. Boyd, and J. M. Dziedzic, "Resonant optical second harmonic generation and mixing," IEEE J. Quantum Electron. **2**(6), 109–124 (1966).
5. E. O. Potma, C. Evans, X. S. Xie, R. J. Jones, and J. Ye, "Picosecond-pulse amplification with an external passive optical cavity," Opt. Lett. **28**(19), 1835–1837 (2003).
6. C. Gohle, T. Udem, M. Herrmann, J. Rauschenberger, R. Holzwarth, H. A. Schuessler, F. Krausz, and T. W. Hänsch, "A frequency comb in the extreme ultraviolet," Nature **436**(7048), 234–237 (2005).
7. R. J. Jones, K. D. Moll, M. J. Thorpe, and J. Ye, "Phase-coherent frequency combs in the vacuum ultraviolet via high-harmonic generation inside a femtosecond enhancement cavity," Phys. Rev. Lett. **94**(19), 193201 (2005).
8. T. Eidam, S. Hanf, E. Seise, T. V. Andersen, T. Gabler, C. Wirth, T. Schreiber, J. Limpert, and A. Tünnermann, "Femtosecond fiber CPA system emitting 830 W average output power," Opt. Lett. **35**(2), 94–96 (2010).
9. A. Cingöz, D. C. Yost, J. Ye, A. Ruehl, M. E. Fermann, and I. Hartl, "Power scaling of high-repetition-rate HHG," in *International Conference on Ultrafast Phenomena*, OSA Technical Digest (CD) (Optical Society of America, 2010), paper MD3.
10. I. Pupeza, T. Eidam, J. Rauschenberger, B. Bernhardt, A. Ozawa, E. Fill, A. Apolonski, Th. Udem, J. Limpert, Z. A. Alahmed, A. M. Azzeer, A. Tünnermann, T. W. Hänsch, and F. Krausz, "Power scaling of a high-repetition-rate enhancement cavity," Opt. Lett. **35**(12), 2052–2054 (2010).
11. J. Kaster, I. Pupeza, T. Eidam, C. Jocher, E. Fill, J. Limpert, R. Holzwarth, B. Bernhardt, T. Udem, T.W. Hänsch, A. Tünnermann, F. Krausz, "Towards MW average powers in ultrafast high-repetition-rate enhancement cavities," in *High Intensity Lasers and High Field Phenomena*, OSA Technical Digest (CD) (Optical Society of America, 2011), paper HFB4.
12. P. Jaegle, *Coherent Sources of XUV Radiation* (Springer, 2006).
13. E. D. Palik, *Handbook of Optical Constants of Solids* (Academic Press, 1998), Vols. 1 and 2.
14. D. C. Yost, T. R. Schibli, and J. Ye, "Efficient output coupling of intracavity high-harmonic generation," Opt. Lett. **33**(10), 1099–1101 (2008).

#146168 - $15.00 USD Received 18 Apr 2011; revised 3 May 2011; accepted 6 May 2011; published 9 May 2011

15. Y.-Y. Yang, F. Süßmann, S. Zherebtsov, I. Pupeza, J. Kaster, D. Lehr, H.-J. Fuchs, E.-B. Kley, E. Fill, X.-M. Duan, Z.-S. Zhao, F. Krausz, S. L. Stebbings, and M. F. Kling, "Optimization and characterization of a highly-efficient diffraction nanograting for MHz XUV pulses," Opt. Express **19**(3), 1954–1962 (2011).
16. K. D. Moll, R. J. Jones, and J. Ye, "Output coupling methods for cavity-based high-harmonic generation," Opt. Express **14**(18), 8189–8197 (2006).
17. A. Ozawa, A. Vernaleken, W. Schneider, I. Gotlibovych, Th. Udem, and T. W. Hänsch, "Non-collinear high harmonic generation: a promising outcoupling method for cavity-assisted XUV generation," Opt. Express **16**(9), 6233–6239 (2008).
18. T. V. Amotchkina, "Empirical expression for the minimum residual reflectance of normal- and oblique-incidence antireflection coatings," Appl. Opt. **47**(17), 3109–3113 (2008).
19. J. A. Dobrowolski, A. V. Tikhonravov, M. K. Trubetskov, B. T. Sullivan, and P. G. Verly, "Optimal single-band normal-incidence antireflection coatings," Appl. Opt. **35**(4), 644–658 (1996).
20. A. V. Tikhonravov, M. K. Trubetskov, T. V. Amotchkina, and J. A. Dobrowolski, "Estimation of the average residual reflectance of broadband antireflection coatings," Appl. Opt. **47**(13), C124–C130 (2008).
21. http://www.optilayer.com/
22. A. V. Smith, B. T. Do, J. Bellum, R. Schuster, and D. Collier, "Nanosecond 1064nm damage thresholds for bare and anti-reflection coated silica surfaces," Proc. SPIE **7132**, 71321T (2008).
23. R. Szipöcs, K. Ferencz, C. Spielmann, and F. Krausz, "Chirped multilayer coatings for broadband dispersion control in femtosecond lasers," Opt. Lett. **19**(3), 201–203 (1994).
24. K. D. Moll, R. J. Jones, and J. Ye, "Nonlinear dynamics inside femtosecond enhancement cavities," Opt. Express **13**(5), 1672–1678 (2005).
25. T. Hänsch and B. Couillaud, "Laser frequency stabilization by polarization spectroscopy of a reflecting reference cavity," Opt. Commun. **35**(3), 441–444 (1980).

1. Introduction

One topic of particular interest in the laser development area is high harmonic generation (HHG) at multimegahertz repetition rates, which opens many promising applications. Attosecond pulse generation [1], high-resolution spectroscopy with XUV frequency combs [2], pump-probe measurements, photoelectron emission microscopy, photoelectron imaging spectroscopy and nanostructure characterization could substantially benefit from XUV MHz-repetition-rate sources. HHG as a common method of generating XUV radiation is made possible by focusing high energy femtosecond pulses into a gas. Because of the high peak intensities ($>10^{13}$ W cm^{-2}) needed for this process, amplifier systems operating at kHz repetition rates are typically used [3]. Due to the very low conversion efficiency (10^{-8}-10^{-6}) of the HHG process and the low average power of kHz driving amplifier systems, the resulting XUV average power is well below the mW level. This fact restricts the field of HHG applications. On the other hand, the use of a high-finesse optical cavity for coherent storage of radiation is a commonly used technique for efficient frequency conversion of cw lasers [4]. This technique was recently extended to mode-locked lasers [5] and has now become widespread in research groups over the world [6,7]. By using the enhancement cavity approach, one can increase the power from a seed mode-locked laser oscillator inside the cavity by a large factor (the enhancement factor, typically 10-10^4). The conditions necessary to realize a large enhancement factor and high average power include the use of high-damage-threshold, thermally-stable intracavity optics with extremely low losses, as well as dispersion control of the cavity.

The first generation of enhancement cavities relied on Ti:sapphire lasers as seeding source, resulting in circulating intracavity pulses of 28 and 60 fs duration and 38 and 480 W average power, respectively [6,7]. Recent development and power scaling of enhancement cavities with Yb-based fiber amplifiers [8] as seeding source approached the 5 kW level for a cavity with an XUV output coupler in it [9] and more than 18 kW for the empty cavity [10]. More advanced cavity designs were proposed to avoid current limitations in further power scaling [11]. At the moment, intracavity-based high harmonic generation is the most promising way of approaching power-scalable compact and coherent XUV MHz repetition rate sources. However, not only can a passive enhancement cavity be considered for increasing the laser power. The opportunity of utilizing high average powers inside the laser oscillator cavity has become a reality with recent progress in high power femtosecond thin disk lasers. Typically, the output coupler transmission T of an oscillator amounts to only a few per cent. This means that power stored inside the oscillator cavity is a factor ~1/T higher than the output power.

#146168 - $15.00 USD Received 18 Apr 2011; revised 3 May 2011; accepted 6 May 2011; published 9 May 2011

When XUV radiation is produced inside the cavity, its output coupling immediately presents a challenge. XUV light is generated collinearly with the driving fundamental laser beam and can easily be absorbed by even 1 μm-thick condensed matter, for instance by the multilayer structure of a mirror, which typically exhibits very poor reflectance of the order of ~10^{-4} at normal incidence [12].

In the following, we would like to summarize the necessary conditions for a cavity XUV output coupler (OC): a) High XUV reflectivity. All XUV light power generated inside the cavity should ideally be coupled out. b) Broad range of XUV reflectance. All generated harmonics of the fundamental driving field (DF) should be collinearly coupled out. c) Losses introduced by the OC for the DF should be low. These losses include absorption, nonlinear effects, depolarization losses and scattering. d) The dispersion introduced by the OC should be small. Nonlinear effects introducing intensity dependent group delay dispersion (GDD) should be small. e) Low thermal lensing (high thermal conductivity and low thermal expansion) is necessary to avoid power dependent resonator stability behavior. f) High damage threshold.

2. Overview of existing XUV output couplers and methods

2.1 Brewster plate

The simplest XUV OC demonstrated so far consists of a plate of good optical quality material that is transparent to the DF and placed at the Brewster angle of incidence inside the enhancement cavity between a focus and a concave mirror, see Fig. 1(a). In this case losses of the p-polarized DF are nearly zero. Due to the difference of the refractive indices of XUV and DF, a small reflection of XUV occurs at the surface of the plate. The reflection of a sapphire plate, used in the previous experiments [6,7], for p-polarized XUV light at the Brewster angle for DF is shown in Fig. 1(b). The optical constants for these calculations were taken from [13].

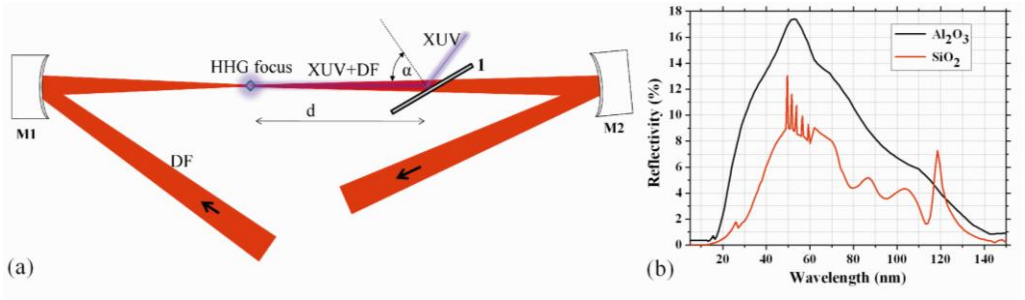

Fig. 1. (a): Brewster plate (1) inside the ring enhancement cavity (shown, only 2 concave mirrors M1, M2 of the cavity). In this case α is equal to the Brewster angle affording lowest losses for circulating DF of p-polarized light. In one of the foci of the cavity (HHG focus), a gas medium (usually a jet) is placed for generating harmonics of DF. Then, XUV and DF co-propagate towards the Brewster plate, where XUV becomes partially reflected out of the cavity whereas DF propagates through the plate without losses and beam distortion. (b): The reflectivity of sapphire (black curve) and fused silica (red curve) plates for p-polarized XUV radiation at the Brewster angle of incidence for 1 μm radiation.

The maximal reflectivity at the wavelength 50 nm amounts to 17% (sapphire) and 10% (fused silica) and strongly decreases for shorter and longer wavelengths, thereby limiting the bandwidth of the OC. It is a difficult task to find optical materials fulfilling conditions a,f above. Materials used in optical applications are usually not sufficiently characterized in the XUV and near-infrared wavelength ranges. To our knowledge, there is no complete data set of material characteristics in the XUV and near-infrared spectrum ranges. The solution implemented is therefore rather a compromise between the XUV reflectivity and the acceptable optical, thermal and nonlinear properties of the Brewster plate material. One of the main limitations of the Brewster plate method is the low XUV out-coupling efficiency and its

#146168 - $15.00 USD Received 18 Apr 2011; revised 3 May 2011; accepted 6 May 2011; published 9 May 2011

relatively narrow bandwidth (conditions a,b). On the other hand, this output coupling method is easy to implement.

2.2 Diffraction grating

An alternative idea consists of an XUV grating etched into the top layer of a highly reflective dielectric coating. The structure acts as a relief grating for XUV light and does not affect the parameters of the DF beam, thus allowing one to avoid any material inside the enhancement cavity and to use only highly reflective optics. The XUV output coupling efficiency in this case is comparable to the Brewster plate method, achieving 10% for 70 nm wavelength [14]. In a relatively narrow wavelength range, the efficiency can be increased by up to 20% by fabricating a blazed XUV grating [15]. With this technique, the maximum intra-cavity power level is limited to 5 kW, by virtue of the damage threshold of the dielectric coating [9]. The physical mechanism of the damage is rather fundamental and is related to the localized electrical field enhancement of the DF at the grating structure, leading to parasitic losses. The proof of this effect is the enhanced third harmonic generation from the surface of such structures discovered in [15]. The spatially dispersed harmonics may make such an XUV OC unsuitable for generation of attosecond pulses. This method thus does not meet the criteria a,b,f.

2.3 Coupling through the hole in a concave mirror

Another method is to drill a small hole in a concave mirror right after the focus (mirror M2 in Fig. 1). XUV light has a smaller divergence in comparison with the DF and can thus be coupled out through this hole. The aperture clips the harmonics of lower orders, thus decreasing the XUV bandwidth of out coupled high harmonics from the long-wavelength side. The hole also introduces losses to the DF and decreases the enhancement factor of the cavity. In this approach it is therefore beneficial to operate the cavity at higher-order transverse modes (e.g. TEM_{01}), having minimal DF at the optical axis in the area of the hole. Even then, the higher order harmonics generated by higher order transverse fundamental radiation will a) be of poor efficiency due to the lower intensity in the focus in comparison with the TEM_{00} mode and b) exhibit a complex spatial profile which may not be applicable for future experiments. So far, this method has shown poor performance in experiment [16].

2.4 Non-collinear HHG

This output coupling method utilizes a completely different scheme of HHG. The technique allows generating high harmonics in a direction which is non-collinear with the driving beam [17]. In this case, two circulating DF pulses inside the cavity overlap temporally and spatially in a gas jet. The XUV light generated is directed along the angle bisector of the two driving beams. The process of non-collinear HHG is poorly investigated and may result in conversion efficiencies much lower than those of a standard HHG with a single fundamental beam. Moreover, the output coupling efficiency of this method is limited by the cavity design [17]. Implementation of this method presents a major challenge.

Among the methods proposed for output coupling the Brewster plate and diffraction grating are the only OCs implemented in enhancement cavities to couple out XUV light.

3. Grazing incidence coated plate (GIP) as an XUV output coupler

The idea of an efficient and broadband XUV OC is similar to the Brewster plate output coupling method: the plate affords the lowest possible losses for DF and some reflection for XUV. In contrast to the Brewster plate, however we propose coating both sides of the plate with an anti-reflection (AR) coating for the grazing incidence of the DF (Fig. 2(a)). At large angle of incidence (>75°), XUV light has drastically increased reflectivity, as follows from the Fresnel equations. This effect can be used to enhance the XUV reflectivity by fabricating a low-loss AR coating for the DF (usually infrared radiation) at both sides of the plate as shown in Fig. 2(a). Typically, fused silica (SiO_2) is used as low refractive index material in multilayer anti-reflection coatings. This material is well studied in both the XUV and near-

#146168 - $15.00 USD Received 18 Apr 2011; revised 3 May 2011; accepted 6 May 2011; published 9 May 2011

infrared wavelength ranges. The optical constants of different types of fused silica were measured and tabulated in [13].

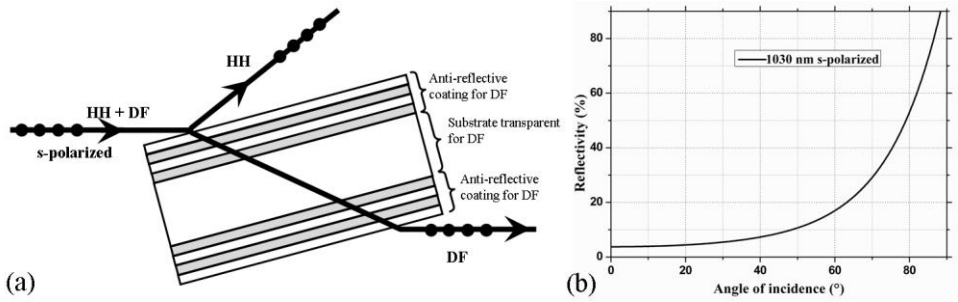

Fig. 2. (a): schematic of the GIP. HH: high harmonics, DF: driving field. (b): Reflectivity of the s-polarized 1030 nm wavelength from fused silica at different angles of incidence.

Fused silica can be chosen as the material of the top layer of the AR coating of the GIP. In Fig. 3, the XUV reflectivity spectra are shown for different grazing incidence angles. At angles of incidence larger than 75° and s-polarized light, the XUV output coupling has reasonable reflectivity (~15%) even at 15 nm wavelength. For the feasible angle of 85°, the reflectivity at a wavelength of 5 nm is expected to be as high as 33%.

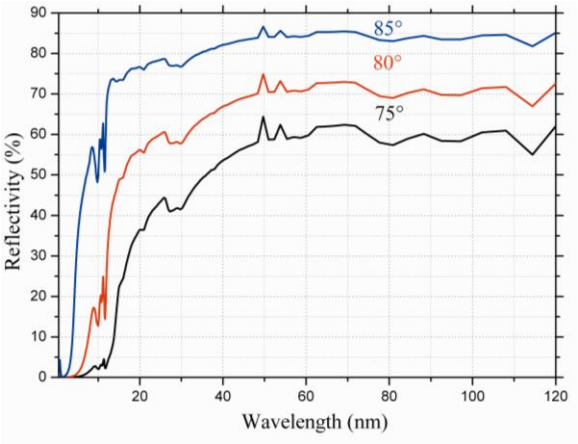

Fig. 3. Calculated spectral reflectivity of SiO_2 for s-polarized XUV radiation at 75°, 80°, 85° angles of incidence. The optical constants were taken from [13].

4. Technical realization of the GIP

Typically, anti-reflection coatings are designed for normal incidence and suppress only a few per cents of the reflectance (in the case of fused silica 4%) at the material-air interface. In this paper we consider an AR coating specifically designed for a large angle of incidence. In publications [18–20] the authors empirically predict a residual reflectance from the AR coating in the case where the total optical thickness and the dispersion of materials and substrates are known. To our knowledge, there is no empirical expression describing the residual reflectance at an angle >75°, and so numerical calculations are needed. In addition, the acceptable angle bandwidth narrows at a large angle of incidence. According to Fig. 2(b), suppression of the reflectance of 50% of the incident light is necessary at angles of incidence around 75-80° in order to achieve a low-loss anti-reflective coating. This is the key criterion in fabricating the proposed anti-reflection coating. Another criterion is to provide low sensitivity of the residual reflection of DF to variation of the incidence angle (the accepted angle of incidence). From the principle of operation, any multilayer coating has an angle

#146168 - $15.00 USD Received 18 Apr 2011; revised 3 May 2011; accepted 6 May 2011; published 9 May 2011

dependent reflection. Due to the divergence of the DF beam incident on the GIP (see Fig. 1), the angles of incidence are different for the central part of DF and its periphery. In the case of a typical cavity, this difference can be as high as 1 ° (ROC of M2 and M1 are 150 mm).

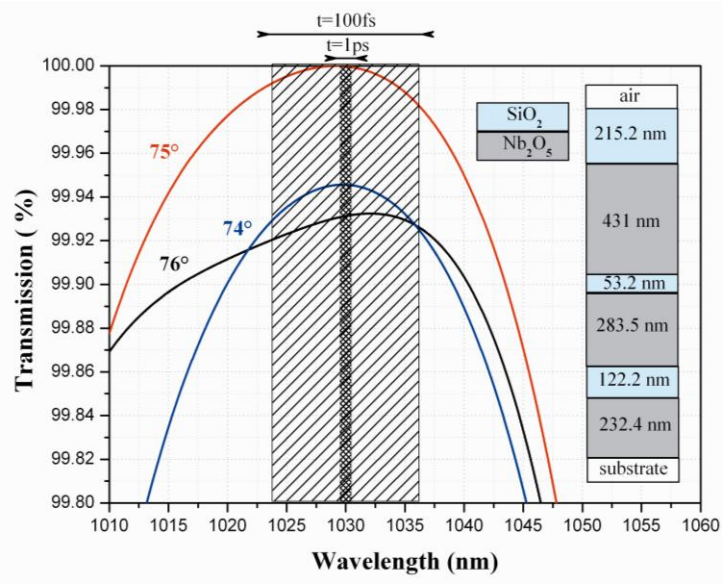

Fig. 4. Transmission of the designed AR coating for different angles of incidence. The AR coating was optimized for 75°. The transmission is shown for one side of the two-side coated substrate. The shaded areas correspond to the spectral width of 1 ps and 100 fs pulses and show the general tendency of the reduced *average* reflection for shorter pulses. The inset shows a multilayer structure of the AR coating.

5. Experiments and discussion

5.1 Fabrication and characterization of the AR coating

For the GIP presented here, the structure of the anti-reflection coating consists of alternating SiO_2 and Nb_2O_5 layers. These materials have the largest difference of low and high refractive indices, and so they were chosen as the optimum choice to achieve low residual reflectivity at grazing incidence [18–20]. The coating was designed with the Optilayer commercial software package [21] for 75° angle of incidence at the central wavelength 1030 nm. The simulated spectral transmission of the coating is shown in Fig. 4 for different angles of incidence. One can see that the losses for the bandwidth-limited $sech^2$-shaped 100-fs pulse corresponding to an 11-nm bandwidth spectrum are below 0.2%. It should be pointed out that a robust design of AR coating consisting of only 3 pairs of SiO_2 and Nb_2O_5 layers was chosen in order to reduce the manufacturing time and corresponding accumulated errors. More complex multilayer structures with broader bandwidth and increased acceptance angle of incidence are possible. To crosscheck this statement, we designed AR coating for 87° angle of incidence and s-polarized light with total losses below 0.1%. This design consists of 30 alternating SiO_2 and Nb_2O_5 layers.

We have produced a magnetron-sputtered (Helios machine, Leybold Optics) AR coating on a high-quality fused silica substrate and performed experimental measurements of its residual reflection for DF. The transmission spectrum was measured with a spectrophotometer (Perkin Elmer, Lambda 950) at 0° angle of incidence and shows good agreement with the calculated transmission curve. At grazing incidence, in order to achieve a good polarization extinction ratio, the laser beam passes a polarizing cubic beam splitter and impinges on the 6-mm thick GIP. The residual reflected DF power from both sides of the GIP is measured with the power meter and amounts to <20 mW of the average power for 10 W of incident power.

#146168 - $15.00 USD Received 18 Apr 2011; revised 3 May 2011; accepted 6 May 2011; published 9 May 2011

Therefore, the residual reflection from both sides of the GIP is less than 0.2%, in good agreement with the calculations (Fig. 4). In order to check the sensitivity of the AR coating to the beam divergence, we focused the beam with a 75-mm lens and measured the residual reflection once again. The reflected power remained the same as in the previous test experiment, thus demonstrating the insensitivity of the coating to the beam divergence in the range of the radius of curvature chosen for the mirrors.

5.2 XUV reflectivity measurements

The reflectivity values expected at such short wavelengths can be reduced because of the surface irregularities, which approach the scale of the XUV wavelength. For instance, the lowest roughness of a fused silica substrate from Layertec GmbH is equal to 0.15 nm and, due to the coating procedure, the roughness can be substantially increased at the upper layer of the GIP surface. Surface imperfections cause scattering of XUV light and result in reduced XUV reflectivity. The GIP coating realized was measured at PTB Bessy to check the influence of coating imperfections and chemical composition on the reflectivity in the XUV range. Figure 5 shows a comparison of the measured and calculated XUV reflectivity of s-polarized radiation in the range from 1 nm to 30 nm at 75° and 80° angles of incidence. In the region from 26 nm to 30 nm the measured reflectivity is around 10% higher. This may be explained by the different chemical compositions of the material tabulated in [13].

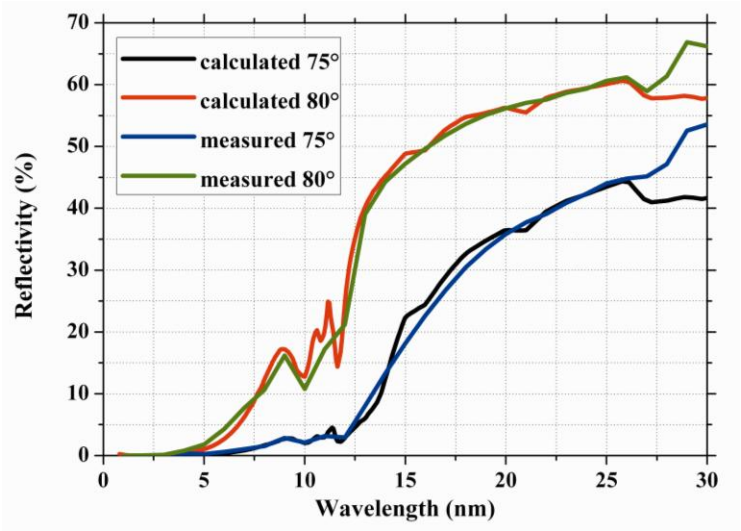

Fig. 5. Comparison between the measured XUV reflectivity and that calculated at 75°, 80° angles of incidence.

Additionally, the measured angle reflectivity at 13 nm wavelength shown in Fig. 6 is in excellent agreement with calculations based on tabulated optical constants. The difference between the measured reflectivity at 30 nm wavelength and that calculated is pronounced especially at small angles of incidence and vanishes at large incidence angles.

The GIP approach allows XUV light to be coupled out in an ultrabroad spectral range. At 80° angle of incidence, the spectral range from 13 nm to at least 120 nm is covered with an efficiency of more than 40% (see Fig. 3). For comparison, the Brewster plate method shows >10% efficiency in the range 30 to 80 nm (Fig. 1, right). Due to the large angle of incidence and s-polarized XUV radiation the reflection spectrum of the GIP can be even more extended, into the VUV range and beyond.

#146168 - $15.00 USD Received 18 Apr 2011; revised 3 May 2011; accepted 6 May 2011; published 9 May 2011

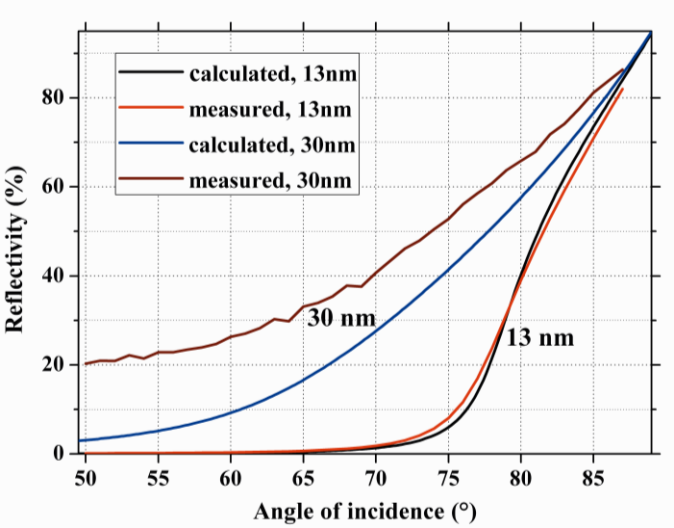

Fig. 6. Measured and calculated angle reflectivities of SiO_2 for s-polarized 13 nm and 30 nm XUV radiation.

5.3 Limitations and extension of GIP to other spectral ranges

The implementation of a GIP inside an enhancement cavity is straightforward. It can be placed between a focus and a concave mirror in a standard symmetric or asymmetric cavity configuration similar to that shown in Fig. 1. An asymmetric cavity configuration (for instance, radius of curvature of the first concave mirror 100 mm and of the second one 200 mm) allows one to extend the distance **d** between the focus and the concave mirror in order to be able to place the GIP closer to the mirror, thus increasing the spot size on it and decreasing the damage probability. Such asymmetric configuration leads to the negligible increase of the beam divergence not influencing the transmission of the GIP. Additionally, due to the large angle of incidence, the size of the beam on the GIP (in the plane of the beam in Fig. 1) will be even larger. For example, for a 2-mm beam at 85° angle, the beam size on the GIP will be as large as 23 mm. It is a nontrivial technological task to make it both thin (thus suppressing nonlinear effects) and of high optical quality. However, the technology of coating very thin (<70 μm) crystals is routinely used in thin disk laser technology and allows high optical quality to be achieved.

The damage threshold of the AR coating has to be addressed as one of the main limitations of power scaling with GIP. An AR coating has a higher damage threshold in comparison with a high reflectance coating containing many layers, and approaches the damage threshold of the bulk material. This fact has been observed in our labs and was proven by others [22]. The specific value of the AR damage threshold is the subject of further investigation. The grazing angle of incidence increases the effective interaction area at the GIP surface and as a consequence reduces the peak intensity at the sample, leading to higher damage threshold.

The GIP provides the possibility of controlling the dispersion via the AR coating. Specially designed AR coating can provide noticeable negative group delay dispersion in transmission, similar to the case with dispersive mirrors [23]. The nonlinear phase of the circulating pulse in a cavity as well as material dispersion can be compensated by a properly designed AR coating. In general, nonlinear effects are a common limitation for all bulk output couplers, which has been investigated in detail [24]. In a GIP, the main contribution to the nonlinear phase is the substrate, due to its thickness in comparison with the AR coating. Not only nonlinear but also thermal effects in a substrate may also limit power scaling. The influence of the thermal effects can be to some extend suppressed in the thin, efficiently cooled GIP. Fused silica as a typical substrate material was chosen for the first proof-of-

#146168 - $15.00 USD Received 18 Apr 2011; revised 3 May 2011; accepted 6 May 2011; published 9 May 2011

principle realization of a GIP. Other prospective materials such as crystalline quartz, CaF_2 and glasses with low absorption (Suprasil 3002) can be used to avoid thermal lensing and nonlinear phase distortions.

The theoretically designed AR coating has a residual reflection of around 40% for p-polarized DF light and has no reflection for the s-polarized light, thus making GIP a polarizer. Polarization sensitivity is a necessary condition for the Hänsch-Couillaud method of locking an enhancement cavity to the seeding oscillator [25]. The XUV radiation generated is polarized parallel to the linearly polarized DF, in our case s-polarized. Delivering the out-coupled XUV beam to the experiment involves further XUV optics, which in general have better reflectivity for s-polarization. In order to realize an enhancement factor around 10^3, the residual GIP losses for DF have to be of the order of 0.05%. Numerical calculations show that this value is attainable and an advanced GIP can be manufactured with modern coating technologies.

As mentioned above, the reflection spectrum of GIP can cover VUV, UV and other spectrum ranges. The reflection of these spectral components should be considered not only from the upper AR layer of GIP as was considered for XUV, but from the whole AR multilayer structure. In our specific case, the upper layer of fused silica starts to become transparent at around 150 nm. Above this wavelength interference between reflections from different alternating layers cannot be neglected. Unfortunately, in our specific case there is a lack of knowledge about the optical constants of Nb_2O_5 below 400 nm. It is worth noting here that by exchanging the alternating material Nb_2O_5 with Ta_2O_5 (the optical constants of this material are known in the spectral range from 150 nm to 8000 nm) the design shown in Fig. 4, has >50% reflectivity in the ranges 135-140, 142-152, 155-175, 185-215, 240-290, 300-315, 380-480, 500-600, 1200-1700 and 2000-3300 nm, and smooth reflectivity >30% in the whole range 3500-8000 nm. By varying designs and materials one can expect other broadband smooth ranges of high reflectivity. New UV-VIS-MIR components can be generated inside the enhancement cavities by using nonlinear crystals instead of a gas medium.

6. Conclusion

We have described an extension of the Brewster plate previously used as an XUV output coupler inside enhancement femtosecond cavities where high harmonics of the fundamental radiation are generated. The proposed GIP, or grazing-incidence coated plate, has low losses for the fundamental light circulating inside the cavity and serves as a highly efficient, extremely broadband output coupler for XUV. Potentially, the short-wavelength reflectivity of GIP can reach the keV range. Due to several advantages the GIP concept allows further power/energy scaling inside the enhancement cavity. Further steps feasible with this concept can cover the VUV-UV spectral ranges and far beyond. GIP can be designed for either s- or p-polarization. Owing to its polarization properties, GIP can be used not only as a dichroic beam splitter but also as a beam combiner or a filter.

Acknowledgments

This work was supported by the Munich Centre for Advanced Photonics (MAP), Photonic Nanomaterials (PhoNa) and KORONA cooperations. The authors would like to thank Ioachim Pupeza for helpful discussions. We also acknowledge the help with the XUV measurements from Christian Laubis and Christian Buchholz from PTB Bessy, Sergiy Yulin and Norbert Kaiser from the Fraunhofer Institute for Applied Optics and Precision Engineering.

#146168 - $15.00 USD Received 18 Apr 2011; revised 3 May 2011; accepted 6 May 2011; published 9 May 2011